ACS OMEGA

http://pubs.acs.org/journal/acsodf

Addition/Correction

Correction to "Effect of Adding Monohydrocalcite on the Microstructural Change in Cement Hydration"

Wanawan Pragot, Ara Carballo-Meilan, Lewis McDonald, Chaiwat Photong, and Waheed Afzal*

ACS Omega **2022**, *7* (41), 36318−36329. DOI: 10.1021/acsomega.2c03977

Cite This: *ACS Omega* 2023, 8, 7242−7242

Read Online

ACCESS | Metrics & More | Article Recommendations

The authorship has changed: Wanawan Pragot regrettably published the work that she carried out during her Ph.D. at the University of Aberdeen under the supervision of Waheed Afzal where this work had been assisted by (then) post-doc Ara Carballo-Meilan and (then Ph.D. student) Lewis McDonald. Wanawan Pragot regrets her action and wants to correct it. She notes that Chaiwat Photong helped her in proofreading the manuscript before she submitted. We believe that the contribution of Chaiwat Photong does not merit being the first author. The revised order and new additions reflect the contributions.

The Acknowledgment and Author contributions have also been revised as given here.

AUTHOR INFORMATION

Corresponding Author

Waheed Afzal − *School of Engineering, University of Aberdeen, King's College, Aberdeen AB24 3UE, United Kingdom;* orcid.org/0000-0002-2927-0114; Email: waheed@abdn.ac.uk

Authors

Wanawan Pragot − *School of Engineering, University of Aberdeen, King's College, Aberdeen AB24 3UE, United Kingdom; School of Energy and Environment, University of Phayao, Phayao, Thailand 56000;* orcid.org/0000-0001-5610-6240

Ara Carballo-Meilan − *School of Engineering, University of Aberdeen, King's College, Aberdeen AB24 3UE, United Kingdom;* orcid.org/0000-0001-6180-1459

Lewis McDonald − *School of Engineering, University of Aberdeen, King's College, Aberdeen AB24 3UE, United Kingdom*

Chaiwat Photong − *School of Energy and Environment, University of Phayao, Phayao, Thailand 56000*

Complete contact information is available at: https://pubs.acs.org/10.1021/acsomega.2c08229

Author Contributions

W.P. prepared an early draft of manuscript with several subsequent revisions by W.A. where A.C.M. and L.M. contributed to expand sections on experimental design and methods. C.P. proofread the near-ready version of the manuscript published, regrettably, without including names of all contributors. W.P. carried out the experiments with a plan from W.A. and help from A.C.M. and L.M. A.C.M. helped to determine the conditions under which different morphologies of carbonate were synthesized. L.M. helped to conduct hydration experiments and helped with XRD.

ACKNOWLEDGMENTS

The authors wish to thank the ACEMAC Facility at the University of Aberdeen for Electron Microscopy, the late Dr. Mohammed Imbabi, and Prof. Fred Glasser for fruitful discussions related to carbon capture, mineralogy, and cement chemistry. Wanawan Pragot acknowledges the Ministry of Science, Technology and Environment, Government of Thailand, for providing her a Ph.D. scholarship to study at the University of Aberdeen where the work was carried out.

Published: February 8, 2023

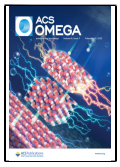

ACS OMEGA

http://pubs.acs.org/journal/acsodf

Article

Effect of Adding Monohydrocalcite on the Microstructural Change in Cement Hydration

Chaiwat Photong and Wanawan Pragot*

Cite This: *ACS Omega* 2022, 7, 36318−36329

Read Online

ACCESS | Metrics & More | Article Recommendations

ABSTRACT: This study explored the application of mineral carbonation products in the form of monohydrocalcite (MHC) as a Portland cement additive. This work studied the effect of adding monohydrocalcite on the microstructural change in cement hydration. We investigated the hydration and microstructure development of MHC−cement at different aging times and different MHC mass % values. Chemical composition changes over time were investigated using X-ray diffraction (XRD) and scanning electron microscopy (SEM). The hydration behaviors of MHC blended with cement were monitored using thermogravimetric analysis and differential thermal analysis (TGA−DTA). The results indicated that the role of MHC in the hydrated cement was enhancing the cement hydration process with may increase the long term strength gain. We also discovered the effect of MHC in term of the long-term chemical reaction and forming the new phase formation of tilleyite in the hydrated MHC cement at long curing ages that was not present in the ordinary Portland cement (OPC) system.

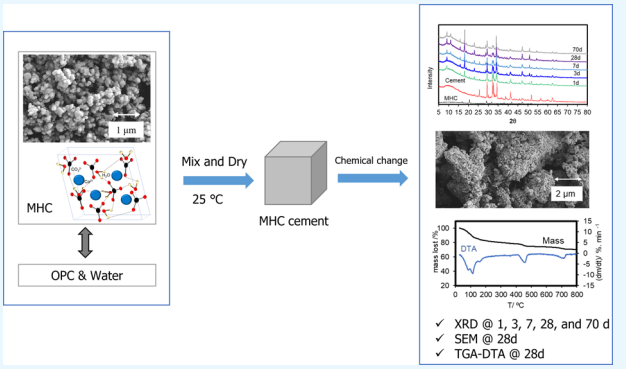

1. INTRODUCTION

Precipitate calcium carbonate (PCC) is one of several products from the mineralization process. PCC is widely used in many different industries, and its market is estimated to reach 98.7 million metric tonnes by 2020.[1] The global market of calcium carbonate products is estimated to grow 96 Mt/year,[1] and the U.K. market for calcium carbonate products is 2 Mt/year.[1] Financial incentives are not the only driving force for PCC production. With at least 37% of CO_2 by mass, PCC offers great potential for CO_2 sequestration. Among its numerous uses, PCC can be used as a clinker substitute for Portland cement. One attractive choice is its use in construction materials, a competitive market with a high demand. PCC may be used along with cement to produce concrete, where PCC can potentially improve certain properties such as the strength of the material rather than acting just as a filler.[2−4] In this regard, products such as PCC produced through the mineral carbonation processes could be a promising alternative to minimize the environmental impact of the cement industry. These products could enter well-established markets with large demand such as cladding in the construction sector, thus partially replacing carbon-intensive products with mineral carbonation products.

The advantage of synthetic $CaCO_3$ or precipitated calcium carbonate (PCC) over $CaCO_3$ produced from natural materials (ground calcium carbonate, GCC) is that PCC can be synthesized with specific requirements in mind based on several properties such as polymorphic composition, morphology, crystal size distribution, surface area, degree of whiteness, brightness, and so on.[5] PCC generally occurs in five stable and crystalline forms, the anhydrous polymorphs (calcite, aragonite, and vaterite) and the metastable hydrated phases (monohydrocalcite, $CaCO_3{\cdot}H_2O$, and ikaite, $CaCO_3{\cdot}6H_2O$).[6−8] There are three dominant dehydrated structures of $CaCO_3$ named calcite, aragonite, and vaterite. Their physical properties are described in Table 1. The most usual and stable form is hexagonal calcite. Orthorhombic aragonite is less abundant, and hexagonal vaterite is the least common of the three.[9] Calcite is precipitated at low temperature and under supersaturation conditions.[9−12] The experimental results from Walker et al.[12] showed aragonite formation under high pressure with an orthorhombic structure. The aragonite structure is transformed from the calcite structure. Figure 1a−c shows the structures of calcite, aragonite, and vaterite. The carbonate group of the calcite structure lies only in a single structure. In the aragonite structure, the carbonate group

Received: June 25, 2022
Accepted: September 21, 2022
Published: October 3, 2022

Table 1. Calcium Carbonate Form[a,b,c,d]

composition	common name	stability	pK_{sp}[d]	physical properties		
				structure	hardness	SP
$CaCO_3$	calcite	stable at atm	8.48	hexagonal[d]	3	2.71
$CaCO_3$	aragonite	stable at high temperature	8.34	orthorhombic, pseudohexagonal[d]	3.5−4	2.95
$CaCO_3$	vaterite	metastable	7.93	hexagonal[d]	3−4	2.95
$CaCO_3$	amorphous calcium carbonate	metastable	N/A	round structure in the metastable phase[d]	none	none
$CaCO_3·H_2O$	monohydrocalcite	stable at atm	7.33	hexagonal[d]	none	2.38
$CaCO_3·6H_2O$	ikaite	stable at low temperature	6.62	monoclinic[d]	none	1.83

[a]atm = atmospheric temperature and pressure. SP = specific gravity. [b]Solubility product constant at 20 °C in pK_{sp} unit ($pK_{sp} = -\log_{10}$).[13,14] [c]Mineralogy. [d]Amorphous calcium carbonate.[15,16]

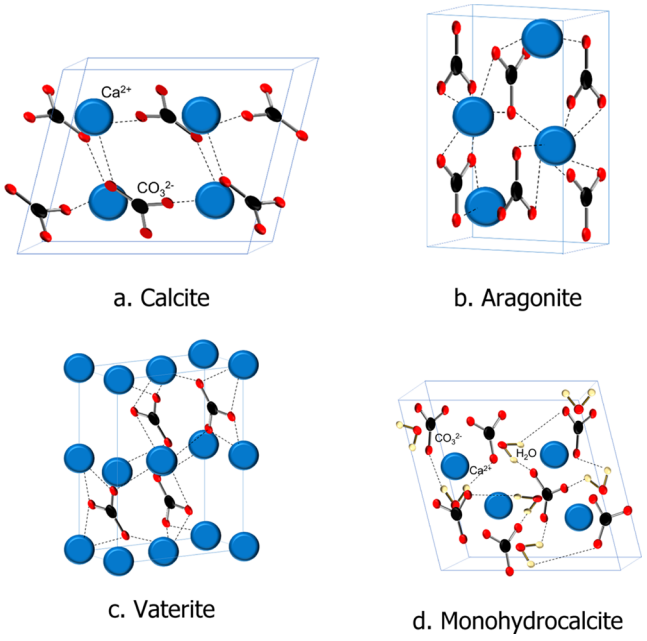

Figure 1. Crystal structure of $CaCO_3$.

lies in two structural planes with the carbonate groups facing opposite directions. Moreover, it was found that temperature affects the form of calcium carbonates, with the tendency to produce aragonite under warm conditions and calcite under cold conditions. From this transformation, it can be observed that aragonite has higher specific gravity than that of calcite and it is less stable than calcite under atmospheric conditions.

Monohydrocalcite (MHC) and ikaite, $CaCO_3·6H_2O$, are hydrated $CaCO_3$ polymorphs that contain water in the structural molecule. MHC can be found in environments where small concentrations of magnesium ions (Mg^{2+}) in the aqueous solution of calcium ions (Ca^{2+}) and carbonate ions (CO^{3-}) are present, such sea water. Ikaite is not found in the nature because it is a metastable form that occurs in cold environments and easily transforms to the stable dehydrated $CaCO_3$ forms such calcite, aragonite, and vaterite.

A rarely considered alternative to the most common mineralization products, such as $CaCO_3$ and $MgCO_3$, is the hydrated $CaCO_3$ polymorph monohydrocalcite (MHC). As a mineralization product, it is interesting for several reasons. First of all, just as calcite, vaterite, and aragonite, it sequesters CO_2 at the same CO_2 to metal oxide ratio of 1:1. Another reason for considering MHC a mineralization product is its frequent presence in laboratory syntheses under a wide range of conditions. MHC is especially common in precipitating environments that contain calcite and inhibiting ions, such as Mg^{2+}.[17−21] It is reasonable to assume that all brines, if they are similar to (or contain) seawater, will have dissolved Mg^{2+}. The presence of small concentrations of Mg^{2+} in the aqueous solution of Ca^{2+} and CO_3^- and moderate pH values can enhance the transformation of $CaCO_3$ into crystalline carbonate polymorphs. Therefore, Mg^{2+} plays a key role in MHC crystallization. The presence of Mg^{2+} can affect the formation of the MHC crystal lattice structure and the water on its surface such as crystal water, absorbed water, and occluded water. Small quantities of Mg^{2+} are incorporated on the MHC lattice structure and facilitate the stabilization of crystal water.[22] The presence of water in MHC makes its structure more open and less dense compared to that of the anhydrous forms of $CaCO_3$ including calcite, vaterite, or aragonite. Thus, the existence of extra water and occluded water could facilitate the increase in the strength of building blocks of MHC and have useful applications in construction.

MHC is stable at room temperature and atmospheric pressure. It has the chemical formulae $CaCO_3·H_2O$ and has a hexagonal crystal structure of $P3_1$, with $a = b = 10.555$ and $c = 7.564$.[23] The crystal structure of MHC is different from that of other precipitated calcium carbonates, calcite,[6] vaterite,[7] and aragonite;[8] the MHC crystal structure has structural water molecules[24] (Figure 1). The atomic structure of MHC consists of irregular 8-folded Ca−O polyhedra, with the central Ca^{2+} surrounded by carbonate groups and structural water molecules. Therefore, there are two types of bonds inside the MHC structure: (1) these structural water and carbonate groups are bonded with ionic bonds between H and O atoms and (2) the bond between the Ca^{2+} atom and carbonate groups. However, there is only one type of bond between the Ca^{2+} atom and carbonate groups for other precipitated calcium carbonates, calcite, vaterite, and aragonite (Figure 1). Based on its solubility product (K_{sp}) at room temperature, MHC ($\log K_{sp} = -7.39$) is more soluble in water than thermodynamically stable calcite ($\log K_{sp} = -8.42$) and metastable aragonite ($\log K_{sp} = -8.22$).

At present, MHC does not have any reported commercial applications. However, MHC has shown promising results in several studies. For instance, MHC was used in remediation to remove arsenic. This material displayed a higher adsorption capacity for arsenic than that of calcite.[20] Furthermore, MHC shares many similarities in chemical composition, precipitation conditions, and thermal behavior to hydrated amorphous calcium carbonate (ACC),[25] a mineral which is already widely utilized in many industries, such as the preparation of structural composite materials.[26]

There are two main mechanisms involved in the hydration of Portland cement: (1) calcium silicate hydrate (C−S−H) system and (2) calcium aluminate and sulfoaluminate system.

https://doi.org/10.1021/acsomega.2c03977
ACS Omega 2022, 7, 36318−36329

On the one hand, in the calcium silicate hydrate system, when Portland cement is mixed with water, the cement particles hydrate and release calcium ions. Calcium and hydroxide ions in the solution react and precipitate calcium hydroxide or portlandite ($Ca(OH)_2$, abbreviated as CH). At the early stage of the hydration process, amorphous silicas such as that from tricalcium silicate or alite (Ca_3SiO_5, abbreviated as C_3S) and dicalcium silicate or belite (Ca_2SiO_4, abbreviated as C_2S) are rapidly hydrated within a few minutes and the hydration continues for days where the equally rapid generation of C−S−H is associated with the increase of cement strength over time.[27] C_3S is responsible for the early strength development. 70% of C_3S will be reacted in 28 days. C_2S is responsible for the late strength development. Only 30% of C_2S will be reacted in 28 days. They constitute 20−40% of cement. Therefore, C_3S and C_2S are responsible for the strength of cement. When C_3S and C_2S are mixed with water, they produce calcium hydroxide ($Ca(OH)_2$, CH) and calcium silicate hydrate ($(CaO)_3(SiO_2)_2 \cdot 4H_2O$, C−S−H).

The reactions of C_3S and C_2S with water (H_2O) are provided below

$$2(Ca_3SiO_5) + 7H_2O \rightarrow (CaO)_3(SiO_2)_2 \cdot 4H_2O + 3Ca(OH)_2 \quad \text{(reaction}$$

$$2(Ca_2SiO_4) + 5H_2O \rightarrow (CaO)_3(SiO_2)_2 \cdot 4H_2O + Ca(OH)_2 \quad \text{(reaction 2)}$$

On the other hand, in the calcium aluminate and sulfoaluminate system, ettringite (AFt, $Ca_6Al_2(SO_4)_3(OH)\text{-}12.26H_2O$) is the main product. Both ettringite and C−S−H can react with CO_2 present in the atmosphere, which can lead to the formation of $CaCO_3$ within the cement matrix.[28−32] Therefore, to prevent the carbonates from being exposed to atmospheric CO_2, the cement samples used in this study were immersed in water during the curing period.

Applications of $CaCO_3$ polymorphs, primarily calcite, have been reported in numerous studies. GCC with large grain size primarily acts as an inert filler in cement due to its nonpozzolanic nature.[33] GCC and PCC with small size can act as an inert filler and/or reactive material.[2−4,34−36] When the amount of calcium is undersaturated, the reaction between calcium-containing phases and tricalcium aluminate (C_3A) of the cement leads to the appearance of a family of phases known as alumina−ferrite−monosulfate (AFm) phases. When calcite is present, calcium hemicarboaluminate $Ca_4Al_2(CO_3)\text{-}0.5(OH)_{13} \cdot 5.5H_2O$ (abbreviated as $CaCO_3$-AFm) forms through a solid-state reaction between C_3A and $CaCO_3$. Calcite behaves as a filler when it is oversaturated and in excess. The amount of excess calcite is usually less than the total amount added because some of it will react.

Recent studies provide important insights into the structure of MHC. It has a more open and less dense structure compared to that of the anhydrous forms of $CaCO_3$ such as calcite, vaterite, or aragonite because of the incorporation of structural water. This water could facilitate an increase in the strength of cement building blocks and decrease the overall water required for hydration of the cement. However, as mentioned earlier, MHC does not have any reported commercial applications and does not have any comprehensive analyses reported on its application in construction materials. Therefore, this study aimed to investigate the effect of adding MHC (monohydrocalcite) on the microstructural change in cement hydration. The study was carried out on samples made from Portland cement paste with and without MHC using water-to-solid ratios (W/C) of 0.5 to observe the hydration process of the MHC-blended cement. The formation of the chemical phases after 1, 3, 7, 28, and 70 days of curing was investigated using X-ray diffraction (XRD) to determine the phase development quantitatively (i.e., unhydrated cement, AFt, CH, C−S−H, and AFm phases). Furthermore, the study included an analysis of the microstructure of the samples. Fragments after 28 days were collected and further characterized with thermogravimetric analysis and differential thermal analysis (TGA−DTA) and scanning electron microscopy (SEM) analysis. Overall, the main objective was to study the influence of MHC on the Portland cement hydration process and therefore determine how feasible this polymorph is as a construction material.

2. MATERIALS AND METHODS

2.1. Materials. *2.1.1. MHC Powder.* MHC powder was synthesized in the laboratory using brine and carbonate solutions. The MHC preparation method is displayed in Figure 2. This synthesis method was decided such that

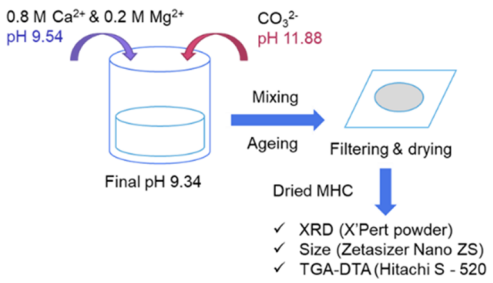

Figure 2. MHC preparation method.

synthetic brines had the same chemical constituents as those of concentrated seawater. The Mg^{2+} concentration was set at 0.2 M, taking into consideration that most of the natural brines were expected to contain at least a small amount of Mg^{2+}.[21,37,21,37] Single-phase MHC was prepared by adding simultaneously 1 M Na_2CO_3 (pH 11.88) and 1 M brine containing 0.2 M $MgCl_2$ and 0.8 M $CaCl_2$ aqueous solution (pH 9.54). Mg^{2+} helps the crystal formation of the hydrated form MHC because the presence of Mg^{2+} can affect the formation of MHC crystal water, absorbed water, and occluded water. Small quantities of Mg^{2+} are incorporated on the MHC lattice structure and facilitate the stabilization of crystal water.[22] After an aging time of 1 h with constant stirring, the precipitate (pH 9.34) was settled, filtered, and rinsed to remove excess NaCl salt and remove all Mg^{2+} in the solution. The filtrate was dried at 40 °C overnight, and its chemical composition was confirmed by XRD (Panalytical X'Pert Pro) that the obtained product was 100% MHC. The XRD patterns of the MHC samples were obtained using a Panalytical X'Pert Pro diffractometer with a reduced range of 5.0065−59.9962° 2θ and a scan time of 16.575 s (Figure 3). The XRD of this pure MHC is depicted in Figure 3. Crystalline MHC constituted spherical particles with crystal agglomeration as shown in Figure 4, as characterized by SEM analysis (Hitachi S-520). The size of MHC is on the nanoscale ranging from 80 to 5000 nm with an average diameter of 380.8 nm, as measured using a Zetasizer Nano ZS (Figure 4). This size of the MHC

https://doi.org/10.1021/acsomega.2c03977
ACS Omega 2022, 7, 36318−36329

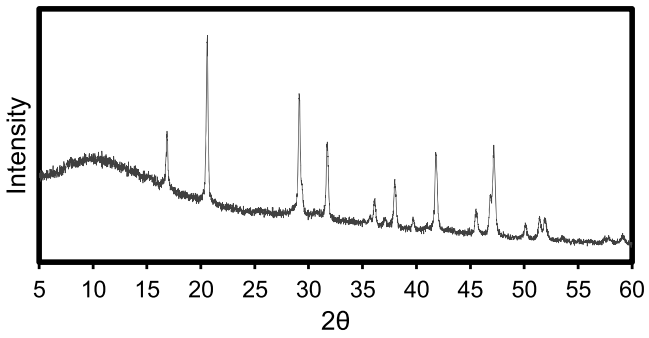

Figure 3. XRD pattern of pure MHC.

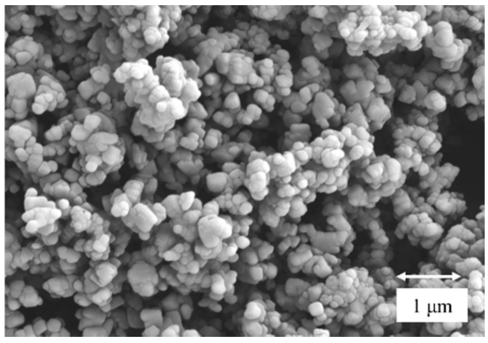

Figure 4. SEM of the synthesized MHC used in this experiment with nanosize varying from 80 to 500 nm.

particles is smaller than the grain size of cement, which can vary from 45 to 300 μm (ASTM C430-9C430-96, ASTM C786-96).

The MHC thermal decomposition behavior was analyzed using thermogravimetric analysis TGA−DTA (STANTON REDCROFT, U.K.). The details of the method for characterizing the thermal decomposition behavior is provided in Section 2.4. The TGA showed a well-established two-step decomposition with a mass loss value of 9.51% at 170 °C and 9.2% at 380 °C. This was in good agreement with the appearance of the DTA endothermic peaks, indicating the MHC structure degradation (Figure 5). These values were nearly equivalent to those calculated from the following reactions: (1) $CaCO_3{\cdot}H_2O \rightarrow CaCO_3 0.5H_2O + 0.5H_2O$ and (2) $CaCO_3 0.5H_2O \rightarrow CaCO_3 + 0.5H_2O$.

2.1.2. Cement. In the case of cement, CEM I 52.5N OPC cement supplied by Hanson Cement UK was used. CEM I 52.5N OPC had a Blaine fineness of 395 m^2/kg. The chemical composition and the oxide contents are given in Tables 2 and 3 that are analyzed by X-ray fluorescence and Bogue calculation.

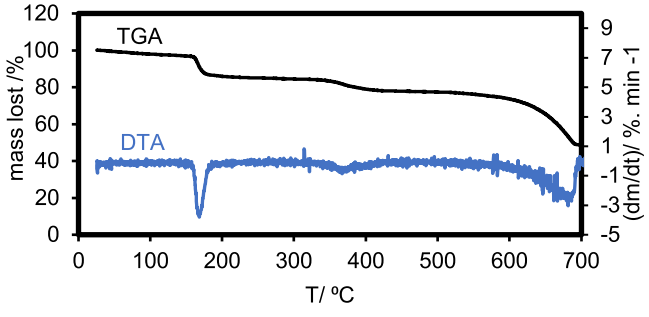

Figure 5. TGA−DTA of pure MHC.

Table 2. Chemical Composition of CEM I 52.5N OPC Cement

phase name[a]	cement chemistry	chemical name	formula	% mass
belite	C_2S	calcium disilicate	Ca_2SiO_4	15.24
alite	C_3S	calcium trisilicate	Ca_3SiO_5	59.65
calcite	$C\bar{C}$	calcium carbonate	$CaCO_3$	4.8
ferrite	C_4AF	tetracalcium aluminoferrite	$4CaO{\cdot}Al_2O_3{\cdot}Fe_2O_3$	8.65
gypsum	$C\bar{S}H_2$	calcium sulfate dihydrate	$CaSO_4{\cdot}2H_2O$	4.65
celite	C_3A	tricalcium aluminate	$3CaO{\cdot}Al_2O_3$	7.01

[a]Cement chemistry' notation: calcium or calcium oxide (CaO) = C, silicon oxide of silica (SiO_2) = S, aluminum oxide or alumina (AlO_3) = A, iron oxide (Fe_2O_3) = F, sulfate (SO_3) = $\bar{S}$, and water (H_2O) = H.

Table 3. Oxide Contents of CEM I 52.5N OPC Cement

oxides	% mass
SiO_2	20.28
Al_2O_3	4.71
Fe_2O_3	3.27
CaO	67.13
SO_3	2.54
MgO	0.67
K_2O	1.40

2.2. Hydrated Cement Preparation Method. The cement and MHC pastes were prepared by manually mixing 600 g of total solids with the desired W/C. Initially, the cement and MHC powder were combined, and then, water was added to the solid mixture and stirred continuously for 2 min. The resulting paste was transferred to three 50 × 50 × 50 mm^3 steel molds. The cubic molds were placed in an oven at a constant temperature of 25 °C. After a setting period of 24 h, the cement cubes were demolded and submerged in a water bath at room temperature for 1, 3, 7, 28, and 70 days to cure. The sample preparation procedure is depicted in Figure 6.

The effect of MHC concentration in hydrated cement was determined by varying the amount of MHC in the paste from 0 to 25% using a constant W/C equal to 0.5. A summary of the composition of each sample is provided in Table 4.

2.3. X-ray Diffraction (XRD) Analysis. The chemical composition of the hydrated cubes prepared at curing times of 1, 3, 7, 28, and 70 days was tested using XRD. The cubes were ground into fine powder before the XRD analysis. The cement and hydrated cement powder were loaded onto standard holders. The test was performed on a Panalytical X'Pert Pro diffractometer equipped with a Cu X-ray source, operating under the following conditions: 40 kV, 45 mA, temperature of 25 °C, step size of 0.0130° 2θ, range of 5.0036−80.9756° 2θ, scan time of 164 s, and continuous scan mode.

The crystalline mineral phases were identified with software X'pert HighScore Plus (PANalytical, NL) using reference patterns from the Crystallography Open Database. Additionally, quantitative analysis was done by applying the Rietveld refinement method to the recorded diffraction patterns. The peak background was removed with 5 bending factors and 10 granularities. The standard deviation is 1% based on the results

https://doi.org/10.1021/acsomega.2c03977
ACS Omega 2022, 7, 36318−36329

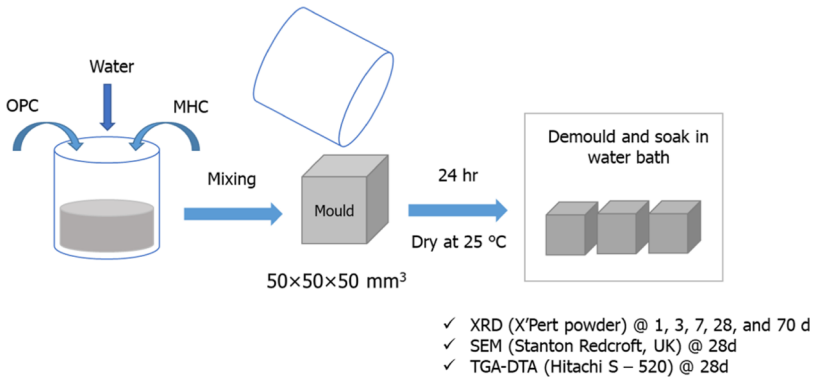

Figure 6. Methodology to determine the role of MHC in cement for construction application.

Table 4. Cement, MHC, and Water Composition Used in the Cement Hydration Study

sample	cement, g	MHC, g	water, g
control, 0% MHC cement 0.5 W/C	600	0	300
5% MHC cement 0.5 W/C	570	30	300
10% MHC cement 0.5 W/C	540	60	300
15% MHC cement 0.5 W/C	510	90	300
20% MHC cement 0.5 W/C	480	120	300
25% MHC cement 0.5 W/C	450	150	300

from the three samples. The additional information for the phases used in the quantitative Rietveld analyses is provided in Table 5.

2.4. Thermal Behavior Characterization. Thermogravimetric analysis (TGA) and differential thermal analysis (DTA) were done using an STA 780 (Stanton Redcroft, U.K.) instrument on the hydrated cement powder cured at 28 days that was ground into a fine powder. The TGA−DTA measurement was carried out using ∼20−30 mg of the sample, weighed into a platinum crucible. The samples were subjected to a dynamic heating rate of 2 °C/min from 25 to 700 °C in a flowing N_2 environment. An alumina sample was used as a DTA reference located in a twin-crucible disk during the characterization.

2.5. Scanning Electron Microscopy (SEM) Image. Prior to analysis by SEM, the samples were pretreated. The 28-day finely hydrated cement samples were dispersed onto ultra-smooth carbon tape and then sputter-coated with a gold−palladium alloy under a flowing argon atmosphere. Once the samples were ready, their morphology was captured visually under a Hitachi S-520 scanning microscope with 20 kV acceleration voltage.

3. RESULTS AND DISCUSSION

3.1. Phase Analysis. XRD analysis was used to follow phase changes within the cement samples over time. For reference, the XRD pattern of a control sample was used. The control sample without MHC and the MHC samples cured for 1, 3, 7, 28, and 70 days are depicted in Figures 7 and 8. The MHC samples contained portlandite (CH), ettringite (AFt, $Ca_6Al_2(SO_4)_3(OH)_{12}{\cdot}26H_2O$), belite or dicalcium silicate (C_2S), calcium hemicarboaluminate ($CaCO_3$-AFm, $Ca_4Al_2(CO_3)0.5(OH)_{13}{\cdot}5.5H_2O$), alite or tricalcium silicate (C_3S), calcite ($C\bar{C}$), and Ferrite (C_4AF) as the main crystalline hydrate and carbonate phases as shown in Table 5.

The results of the sample without MHC defined as hydrated control cement sample without MHC after cured at 1, 3, 7, 28, and 70 days are provided in Figure 7 and Table 6. Figure 6 showed XRD pattern of hydrated control cement sample without MHC cured at 1, 3, 7, 28, and 70 days. The results of the quantitative analysis achieved with the Rietveld refinement method can be seen in Table 6. The amount displayed in the table corresponded to the percentage of each phase in the sample.

The results indicated that after the cement mixed with water, the C_3S and C_2S react with water and create CH and C−S−H phase in the calcium silicate hydrate (C−S−H) system (reactions 1 and 2). These effect to the reduction of the C_3S and C_2S phase in the cement at longer curing time as present in Table 6. The CH decreased due to the reaction with CO_2 in the air and carbonate in the cement to produce $C\bar{C}$. When mixed with water C_3A produce ettringite (AFt) and mono sulfate hydrate (AFm). Since C−S−H is the gel like material, the formation can be varied and give different proportion of CH, AFm, and AF during this cement hydration phase.

Table 5. Additional Information for the Phases Used in the Quantitative Rietveld Analyses

phase name	cement chemistry	chemical formula	ICSD[a] code
MHC		$CaCO_3{\cdot}H_2O$	100847
calcite	$C\bar{C}$	$CaCO_3$	80869
portlandite	CH	$Ca(OH)_2$	202220
belite	C_2S	Ca_2SiO_4	81097
alite	C_3S	Ca_3SiO_5	94742
ferrite	C_4AF	$4CaO{\cdot}Al_2O_3{\cdot}Fe_2O_3$	161525
calcium hemicarboaluminate ($CaCO_3$-AFm)	AFm	$Ca_4Al_2(CO_3)0.5(OH)_{13}{\cdot}5.5H_2O$	41-0221
ettringite	AFt	$Ca_6Al_2(SO_4)_3(OH)_{12}{\cdot}26H_2O$	155295
tilleyite		$Ca_5(Si_2O_7)(CO_3)_2$	14256

[a]ICSD = Inorganic Crystal Structure Databases.

https://doi.org/10.1021/acsomega.2c03977
ACS Omega 2022, 7, 36318−36329

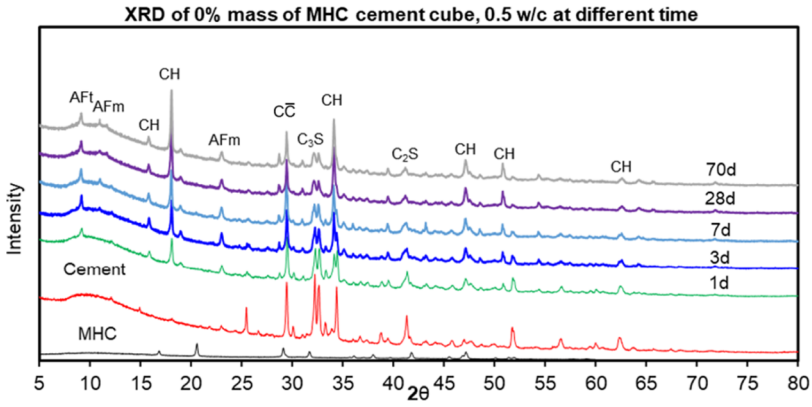

Figure 7. XRD pattern of hydrated control cement sample without MHC cured at 1, 3, 7, 28, and 70 days.

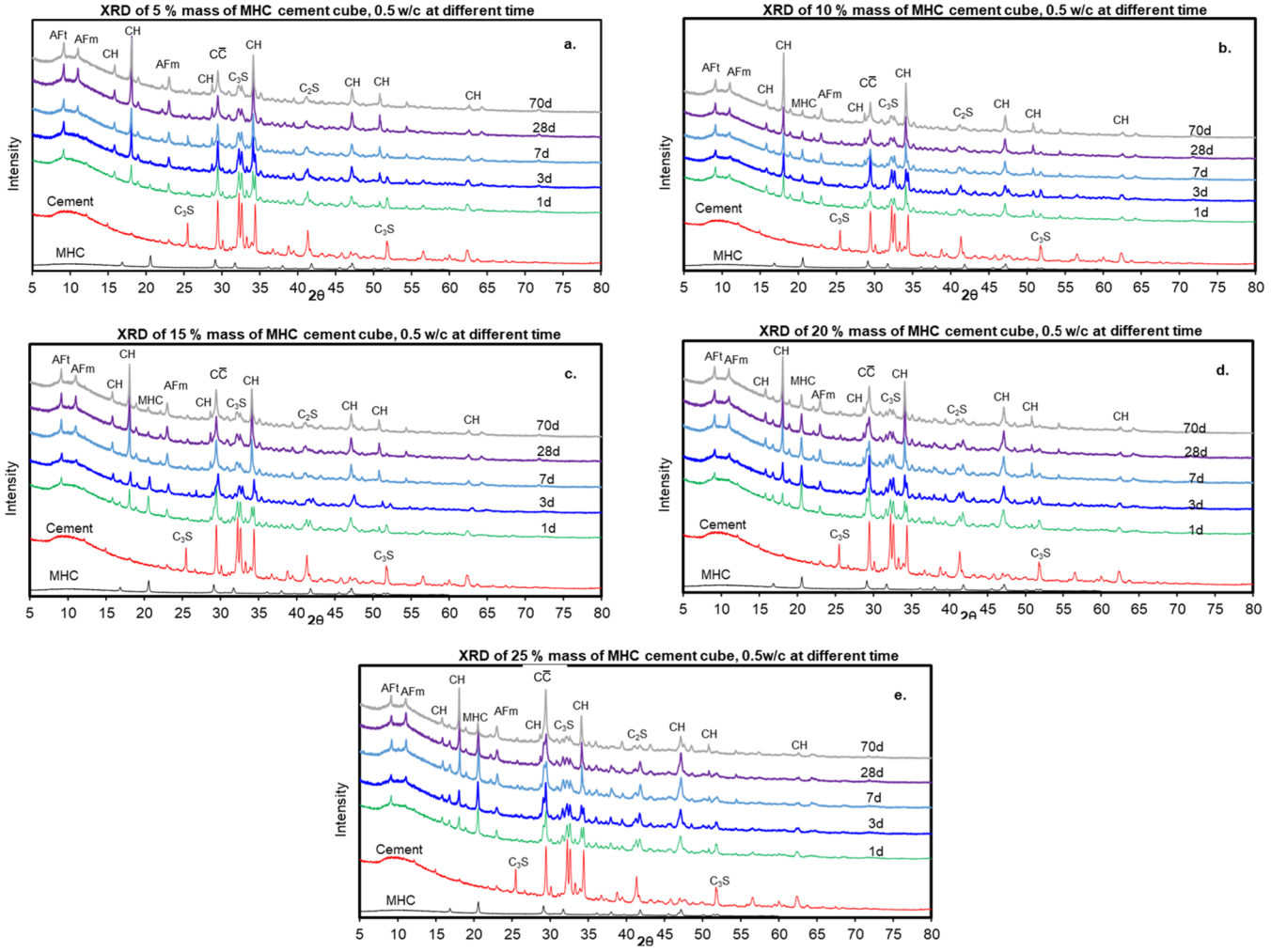

Figure 8. XRD pattern of 1, 3, 7, 28, and 70 days hydrate cement samples with 0.5 W/C containing MHC at (a) 5% mass of MHC, (b) 10% mass of MHC, (c) 15% mass of MHC, (d) 20% mass of MHC, (e) 25% mass of MHC.

A reduction of the C_3S phase paired with an increase in the intensity of the CH and AFt peaks. Due to its amorphous nature, the formation of C−S−H was not recorded using XRD analysis. The AFt phase was seen to form after 1 day of curing when the cement paste started to solidify. A maximum was reached at day 3 of curing and afterward its amount decreased steadily. This observation could be related to the reaction between the carbonate ions and ettringite[40]. We monitored the change of AFm phase in the form of calcium hemi-carboaluminate ($CaCO_3$-AFm). The slight increase in the intensity of the $CaCO_3$-AFm peaks could be attributed to the chemical reaction between the reactive $CaCO_3$ and the C_3A of the cement. Furthermore, the relative intensity of C_4AF hydration are similar C_3A by forming AFt in the presence of gypsum. However, hydration this C_4AF is much slower than hydration of C3A that confirmed by the amount remained almost the same for 28 days as shown in Table 6 and disappeared at 70 days. In cement, if there is insufficient

https://doi.org/10.1021/acsomega.2c03977
ACS Omega 2022, 7, 36318−36329

Table 6. Chemical Composition of the Control Samples Using 0.5 W/C of Hydrated Cement at Different Curing Time and Characterized by XRD

	curing time (days)				
phase	1	3	7	28	70
AFt	11.9	23	17.3	17.7	19.3
CH	19.2	17.3	14.1	10.7	39.1
C_2S	18.4	16.6	14.3	15	4.8
$CaCO_3$-AFm	2.9	3.5	3.7	8.7	11.1
C_3S	37.7	22.7	17.5	20.1	0.0
$C\bar{C}$	5	13.6	24.6	23.2	22.8
C_4AF	4.9	3.3	8.5	4.7	0.0

gypsum to convert all of the C_4AF to ettringite, then an iron-rich gel forms at the surface of the silicate particles which is proposed to slow down their hydration.

After that the effect of MHC concentration in hydrated cement was determined by varying the amount of MHC into the paste from 5 to 25% using a constant W/C equal to 0.5 as summarized the mixing in Table 4. The cement containing MHC was then analyzed the chemical composition using XRD. The XRD pattern of the hydrated cement samples containing MHC is shown in Figure 8. The samples were cured for 1, 3, 7, 28, and 70 days and contained CH, AFt, C_2S, $CaCO_3$-AFm, C_3S, $C\bar{C}$, C_4AF, and tilleyite as part of their crystalline composition as presented. The The results of the quantitative analysis achieved with the Rietveld refinement method can be seen in Figure 9.

The hydrate cement samples with MHC has the hydration reaction. Clearly seen the reduction of the amount of C_3S and C_2S with time resulted to their chemical reaction with water to form other phases. This is similar to the results of the control in Table 6 and Figure 7. Another similarity with the control sampling is the amount of ferrite (C_4AF) decreased as the curing time increased indicating the formation of C_4AF to AFt.

Significant differences were observed between the crystalline composition of the specimens obtained from the control (Figure 7) and the hydrated cement samples containing MHC (Figures 8 and 9), in both cases at different curing times. The quantity of CH, the hydration product of cement and water, is high for hydrate cement samples containing 5 and 10% mass of MHC. For hydrate cement samples containing 15−25% mass of MHC have low quantity of CH phase. This might be possible to the calcium hydroxide hydrolyzed with the water in MHC and releases the calcium ions in released and form C−S−H gel and AFt and AFm phases. From this reason the amount of AFt and AFm phase are considerable higher for the hydrate cement samples at longer curing time as compared to the lower curring. There are two possible reasons for this. The first reason that could explain this finding is that MHC could partially react with C_3A of the cement and transforms into $CaCO_3$-AFm. Secondly, the interaction of the water structure in MHC with the C_3A phase may have led to a more rapid formation of AFt and $CaCO_3$ by donating its structural water to the cement for the cement hydration process. The MHC was consumed and the phase all disappeared for hydrate cement samples containing 5% MHC after 1 day of curing. This could be attributed to the cement hydration process and

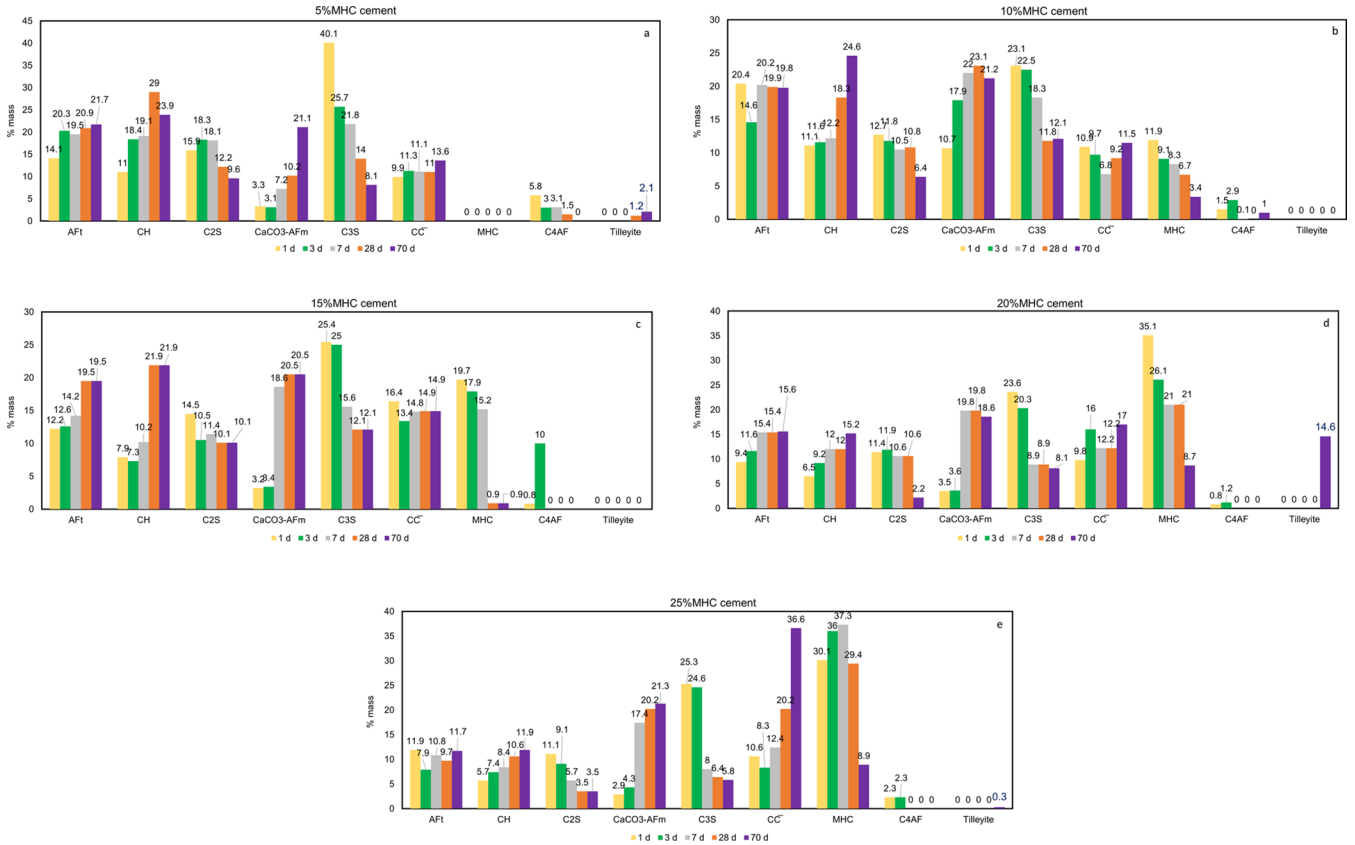

Figure 9. Chemical composition of the hydrated cement containing MHC prepared with 0.5 W/C at different curing times in days (d) at (a) 5% mass of MHC, (b) 10% mass of MHC, (c) 15% mass of MHC, (d) 20% mass of MHC, (e) 25% mass of MHC.

https://doi.org/10.1021/acsomega.2c03977
ACS Omega 2022, 7, 36318−36329

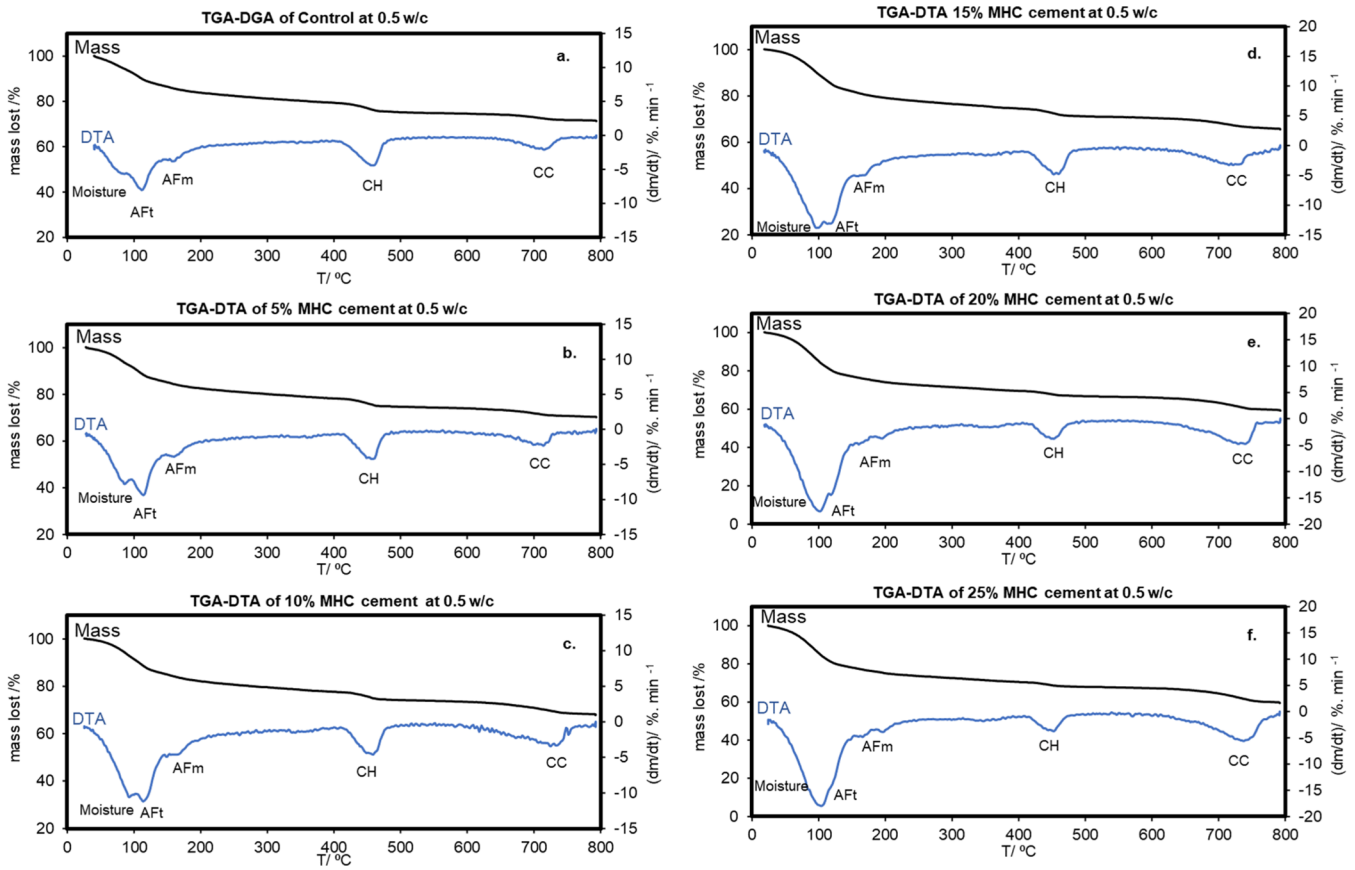

Figure 10. TGA−DTA of hydrated cement samples with 0.5 W/C and containing different amounts of MHC: (a) 0% mass of MHC, (b) 5% mass of MHC, (c) 10% mass of MHC, (d) 15% mass of MHC, (e) 20% mass of MHC, (f) 25% mass of MHC.

how the structural water in MHC was used and transformed into calcite. This can be observed in the amount of calcite at 1 day of curing was 9.9% mass, a value higher than the control, 5% mass. Hydrated cement samples containing initial amounts of MHC greater than 10% mass (Figure 7b−e) exhibited residual amounts and this MHC content was reduced considerably with the curing time. This was possible because the hydrated samples were oversaturated with MHC, and for this reason MHC acted as a filler. The role of MHC as a reactive chemical was detected by the increase in the quantity of the hydration and carbonation products such as AFt, CH, $CaCO_3$-AFm, and $C\bar{C}$ if we compare these compositions with the ones obtained from the control samples. Therefore, MHC enhanced the rate of hydration of the cement samples. Moreover, a faster rate of formation of CaCO3-AFm is evidenced due to the interaction of MHC with calcium aluminate hydrates of cement pastes and the same pattern is also found in other studies of limestone and cement.[2,3,33−35,38−41] In that case, as the residual water of from MHC are still available, hydration continues and the induction period gives way to the third phase of hydration, the acceleratory period and this might lead to the long term strength gain or the other chemical reaction and a new phase formation.[2,40,41] From that reason, this study found that the samples containing an initial mass of MHC has another interesting observation of the formation of tilleyite, chemical formula $Ca_5(Si_2O_7)(CO_3)_2$, a new additional phase of tilleyite in some MHC cement samples (Figure 9a,d,e) at longer curing times, not observed in the control samples (sample without MHC). The slightly tilleyite peaks, at the position of 29.0803, 29.0804, 29.6923, 29.7677, 30.3202, 43.0853, and 49.1523° 2θ, were accelerated with other phases and quantity was analyzed using the software X'pert HighScore Plus (PANalytical, NL) using reference patterns from the Crystallography Open Database. The phase tilleyite was measured at 28 and 70 days of curing where it was formed out of the reaction between the cement and the residual MHC after calcite transformation at longer curing times for some hydrated cement with MHC samples, for example in hydrated cement with 5% mass of MHC samples (Figure 9a) contained tilleyite 1.2% mass for 28 days of curing and 2.1% mass for 70 days of curing. This tilleyite phase is uncommon and also reported the as the novels phase from the amorphouse calcium carbonate, nano scale calcite, and micro scale calcite chemically reaction with C−S−H in the cement during hydration reaction of cement.[40,41] These studies indicated that the using of nano-size calcium carbonate blended cement effect to the chemical formation of tilleyite in the hydrated mineralogy.

3.2. Thermal Decomposition Analysis. A comparison between the chemical phases formed in the cement samples cured for 28 days and their thermal degradation was done using TGA−DTA. The thermal characterization was based on mass losses at specific temperature ranges. The temperature range between 25 and 300 °C induces the decomposition of physisorbed moisture, C−S−H, AFt and AFm. In the temperature range of 300−500 °C, CH decomposes in cement pastes containing carbonated material. Thus, the mass loss between 25 and 500 °C can be used to identify the total dehydration of the hydrated cement products. As the temperature continues to rise, the mass lost after 500 °C is

https://doi.org/10.1021/acsomega.2c03977
ACS Omega 2022, 7, 36318−36329

attributed to the decarbonization of calcium carbonate and indicates the loss of bonded CO_2 on the hydrated cement samples.[42] The temperature for decarbonization can be used to differentiate the crystalline calcium carbonates. When the carbonate decomposes from 550 to 720 °C this generally suggests a poor-crystalline phase and its decomposition from 720 to 960 °C indicates a well-crystalline phase.[43]

Figure 10 presents the TGA−DTA results of the hydrated MHC cement samples containing 0.5 W/C and the curing time was 28 days. The effect of the MHC concentration in the cement samples was measured using different mass percentages. The TGA curves of every sample showed a decomposition occurring in 3 steps: the first step at 100 °C, followed by a second step at 450 °C and a last step of mass lost at 750 °C. The loss of water at 25−500 °C corresponded to the moisture content whereas the mass loss after 500 °C related to the CO_2 loss.[44]

The DTA results describe the endothermic thermal degradation of cement products with and without MHC. A comparison between control samples and samples using 5−25% mass of MHC (Figure 10) was done using DTA characterization at a broad temperature range. Results indicated a sharper reduction of DTA in the samples containing MHC cement (Figure 10b−10f), not seen in the control (Figure 10a). This points out that even a small amount of MHC in the cement is enough to affect the structure of the binding phase. At a temperature range between 25 and 200 °C, three endothermic DTA peaks were found. The three components from the thermal degradation in the region under study were:[30] (1) structural water, (2) AFt, and (3) AFm. The DTA of structural water and AFt was marked by the prominent DTA endothermic peak at a temperature range of 25 and 150 °C. This peak was greater in the cement samples containing higher amounts of MHC indicating that MHC leads to the formation of more phases containing structural water and AFt. The amount of ettringite in the samples was greater than the measured structural water in the hydrated cement products containing 0−10% mass of MHC. However, this trend was reversed when the amount of MHC in the sample was above 15% mass (more structural water than ettringite was observed). This later case is more favorable. The excess in structural water is useful for the long-term formation of cement hydrate products because it can ensure that the water is sufficient for the hydration process.[45] The small endothermic DTA degradation peak of AFm was observed between 150 and 200 °C. No apparent differences were observed in this AFm peak with variations in the MHC content. The second step mass loss step between 450 and 500 °C coincides with an endothermic peak is the CH degradation indicating the structural thermal degradation of hydroxy group on CH. The calcium carbonate degradation appeared during the last mass loss at 750 °C. The carbonated decomposition took place at high temperatures illustrates the possible high thermal stability and high crystallinity of the calcium carbonate phase. The decomposition of the hydration products is summarized in Figure 11. The mass of CO_2 lost due to decarbonation is summarized in Figure 12.

Figure 11 shows the mass loss between 25 and 500 °C in the hydrated cement products under the presence and absence of MHC and with a constant water content (0.5 W/C). The mass loss between 25 and 300 °C represented the amount of structural water, AFt and AFm. Their increase was positively correlated with the addition of higher amounts of MHC in the

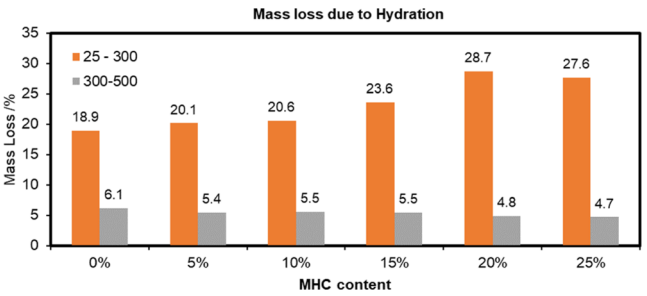

Figure 11. Water loss in the cement sample with/without MHC at 0.5 W/C.

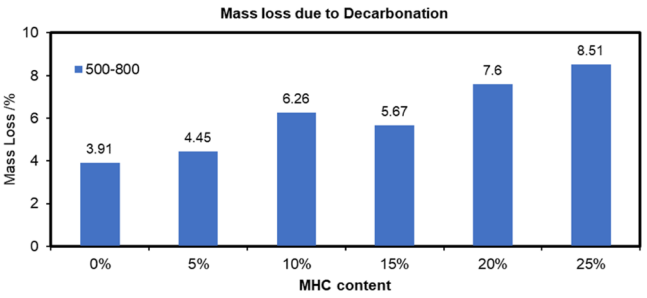

Figure 12. CO_2 loss in the hydrated cement with/without MHC at 0.5 W/C.

cement preparation. On the contrary, the amount of CH decreased with an increase in the MHC content. These two trends were in good agreement with the DTA characterization.

Figure 12 depicts the effect of the initial amount of MHC in the hydrated cement samples (0.5 W/C) on the CO_2 loss content. It is self-evident that cement samples containing more MHC showed a greater carbon content compared to the control sample where this calcium carbonate polymorph was absent. The two possible routes of calcium carbonate formation within the sample could be: (1) the transformation of C−S−H and CH into $CaCO_3$, and (2) the formation of MHC when its structural water participated in the cement hydration process.

Addition of MHC influenced the hydration and carbonation reactions of hydrated cement sample and revealing the role of MHC as the reactive material. The filler effect of MHC is associated with its particle size (size of 380.8 nm). The finer MHC is related to higher packing density. The reactive effect is influenced by the amount of residual MHC in the hydrated MHC blended cement sample. TGA−DTA analysis revealed that the introduction of MHC tended to increase the formation of hydration components (especially C−S−H). As the hydration component is the main factor to the long term compressive strength gain in the cement,[2,4,28,30,36,41,46,47] this MHC adding could be influence to the compressive strength of the hydrated cement. Substitute of cement with MHC decreases the water to react with cement particles, while the chemical effect may resulted in the increase of strength and new phase forming (tillyite).

3.3. SEM. SEM characterization was performed on samples with different MHC contents. Results revealed four distinctive structures on the surface of the hydrated cement samples: plate-shaped, cloud like, needles, and spherical structures.[48] Plate-shaped structures were identified as calcium hydroxide or portlandite (Figure 13a). Cloud-like structures were assigned to the C−S−H phase. Needle-like and spherical structures

https://doi.org/10.1021/acsomega.2c03977
ACS Omega 2022, 7, 36318−36329

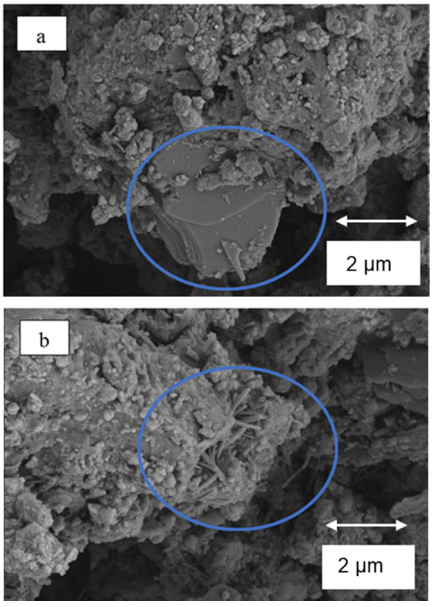

Figure 13. SEM of control at 28 days curing time showing the distinctive shapes of (a) portlandite (CH) and (b) ettringite (AFt).

were found to be ettringite (Figure 13b). After 28 days of hydration, C−S−H was the dominant phase as suggested by the cloud like structure covering all the particles (Figures 14

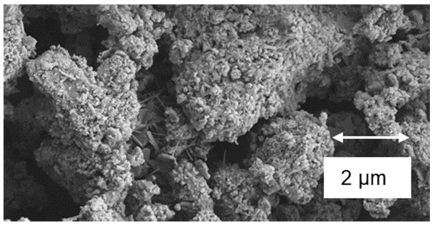

Figure 14. SEM showing some of ettringite and portlandite structure of a sample with 20% mass of MHC cured at 28 days.

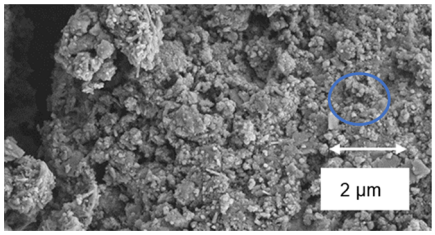

Figure 15. SEM showing some of ettringite, portlandite and small size calcite structure in a cement sample with 20% mass of MHC at 28 days of curing.

and 15) with some calcium hydroxide was detected in each sample. The SEM analysis corroborated the formation of the hydration phases already identified by the XRD and TGA−DGA characterizations.

4. CONCLUSIONS

An effect of adding monohydrocalcite on the microstructural change in cement hydration was studied in this paper. The results could be applied for the use of MHC on a commercial scale as MHC proved to be an alternative product for cement clinker substitution as it showed a dual role in the hydrated cement paste, both as filler and as a reactive material. The MHC acts as filler when the quantity added is more than 10% of the mass of the cement sample resulting in the oversaturation of MHC in the sample after curing. The addition of MHC enhanced the rate of hydration reactions of cement constituents and lead to the formation of tilleyite, a rarely reported hydration product at ambient temperatures. Replacement of cement with MHC increased the water available to react with cement particles that could be beneficial for the long-term strength development and reduce the water required for complete hydration. The MHC could have potential benefits on its applicability in the construction sector and seems advantageous based on the current findings about of the effect of adding monohydrocalcite (MHC) on the microstructural change in cement hydration the chemical composition changes of cement. As the compressive strength and flexural strength are the importance parameters for the cement mechanical properties, the future work should be undertaken on the effect of addition of calcite monohydrate.

AUTHOR INFORMATION

Corresponding Author

Wanawan Pragot − *School of Energy and Environment, University of Phayao, Phayao 56000, Thailand;* orcid.org/0000-0001-5610-6240; Email: wanawan.pr@up.ac.th

Author

Chaiwat Photong − *School of Energy and Environment, University of Phayao, Phayao 56000, Thailand*

Complete contact information is available at: https://pubs.acs.org/10.1021/acsomega.2c03977

Author Contributions

The manuscript was written through contributions of all authors. W.P. carried out work and wrote the paper. C.P. reviewed and edited the writing. All authors have given approval to the final version of the manuscript.

Notes

The authors declare no competing financial interest.

ACKNOWLEDGMENTS

The authors wish to acknowledge Dr. Lewis J. McDonald and Dr. M. Ara Carballo-Meilan to share their experience and give the good advice for my work-life balance and emotional support.

REFERENCES

(1) Pieri, T.; Nikitas, A.; Castillo-Castillo, A.; Angelis-Dimakis, A. Holistic Assessment of Carbon Capture and Utilization Value Chains. *Environments* **2018**, *5*, 108.

(2) McDonald, L.; Glasser, F. P.; Imbabi, M. S. A New, Carbon-Negative Precipitated Calcium Carbonate Admixture (PCC-A) for Low Carbon Portland Cements. *Materials* **2019**, *12*, No. 554.

(3) Ma, J.; Yu, Z.; Ni, C.; Shi, H.; Shen, X. Effects of Limestone Powder on the Hydration and Microstructure Development of Calcium Sulphoaluminate Cement under Long-Term Curing. *Constr Build. Mater.* **2019**, *199*, 688−695.

(4) Matschei, T.; Lothenbach, B.; Glasser, F. P. The Role of Calcium Carbonate in Cement Hydration. *Cem. Concr. Res.* **2007**, *37*, 551−558.

https://doi.org/10.1021/acsomega.2c03977
ACS Omega 2022, 7, 36318−36329

(5) Lippiatt, N.; Ling, T. C.; Pan, S. Y. Towards Carbon-Neutral Construction Materials: Carbonation of Cement-Based Materials and the Future Perspective. *J. Build. Eng.* **2020**, *28*, No. 101062.
(6) Graf, D. Crystallographic Tables for the Rhombohedral Carbonates. *Am. Mineral.* **1961**, *46*, 1283−1386.
(7) De Villiers, J. P. R. Crystal structures of aragonite, strontianite, and witherite. *Am. Mineral.* **1971**, *56*, 758−767.
(8) Wang, J.; Becker, U. Structure and Carbonate Orientation of Vaterite ($CaCO_3$). *Am. Mineral.* **2009**, *94*, 380−386.
(9) Nehrke, G.; Poigner, H.; Wilhelms-Dick, D.; Brey, T.; Abele, D. Coexistence of Three Calcium Carbonate Polymorphs in the Shell of the Antarctic Clam Laternula Elliptica. *Geochem., Geophys., Geosyst.* **2012**, *13*, No. Q05014.
(10) Pan, S. Y.; Chiang, P. C.; Chen, Y. H.; Chen, C.; Lin, H. Y.; Chang, E. E. Performance Evaluation of Aqueous Carbonation for Steelmaking Slag: Process Chemistry. *Energy Procedia* **2013**, *37*, 115−121.
(11) Chhim, N.; Kharbachi, C.; Neveux, T.; Bouteleux, C.; Teychené, S.; Biscans, B. Inhibition of Calcium Carbonate Crystal Growth by Organic Additives Using the Constant Composition Method in Conditions of Recirculating Cooling Circuits. *J. Cryst. Growth* **2017**, *472*, 35−45.
(12) Walker, J. M.; Marzec, B.; Nudelman, F. Solid-State Transformation of Amorphous Calcium Carbonate to Aragonite Captured by CryoTEM. *Angew. Chem., Int. Ed.* **2017**, *56*, 11740−11743.
(13) Schall, J. M.; Myerson, A. S. Solutions and Solution Properties. *Handb. Ind. Cryst.* **2019**, *7*, 1−31.
(14) Dean, J. A.*Lange's Handbook of Chemistry*, 15th ed.; McGraw-Hill Education LLC, 1999.
(15) Blue, C. R.; Giuffre, A.; Mergelsberg, S.; Han, N.; De Yoreo, J. J.; Dove, P. M. Chemical and Physical Controls on the Transformation of Amorphous Calcium Carbonate into Crystalline CaCO3 Polymorphs. *Geochim. Cosmochim. Acta* **2017**, *196*, 179−196.
(16) Han, Y. S.; Hadiko, G.; Fuji, M.; Takahashi, M. Influence of Initial CaCl2 Concentration on the Phase and Morphology of CaCO3 Prepared by Carbonation. *J. Mater. Sci.* **2006**, *41*, 4663−4667.
(17) Bots, P.; Benning, L. G.; Rodriguez-Blanco, J. D.; Roncal-Herrero, T.; Shaw, S. Mechanistic Insights into the Crystallization of Amorphous Calcium Carbonate (ACC). *Cryst. Growth Des.* **2012**, *12*, 3806−3814.
(18) Michel, F. M.; MacDonald, J.; Feng, J.; Phillips, B. L.; Ehm, L.; Tarabrella, C.; Parise, J. B.; Reeder, R. J. Structural Characteristics of Synthetic Amorphous Calcium Carbonate. *Chem. Mater.* **2008**, *20*, 4720−4728.
(19) Konrad, F.; Purgstaller, B.; Gallien, F.; Mavromatis, V.; Gane, P.; Dietzel, M. Influence of Aqueous Mg Concentration on the Transformation of Amorphous Calcium Carbonate. *J. Cryst. Growth* **2018**, *498*, 381−390.
(20) Fukushi, K.; Munemoto, T.; Sakai, M.; Yagi, S. Monohydrocalcite: A Promising Remediation Material for Hazardous Anions. *Sci. Technol. Adv. Mater.* **2011**, *12*, No. 064702.
(21) Nishiyama, R.; Munemoto, T.; Fukushi, K. Formation Condition of Monohydrocalcite from CaCl2-MgCl2-Na2CO3 Solutions. *Geochim. Cosmochim. Acta* **2013**, *100*, 217−231.
(22) Liu, R.; Liu, F.; Zhao, S.; Su, Y.; Wang, D.; Shen, Q. Crystallization and Oriented Attachment of Monohydrocalcite and Its Crystalline Phase Transformation. *CrystEngComm* **2013**, *15*, 509−515.
(23) Swainson, I. P. The Structure of Monohydrocalcite and the Phase Composition of the Beachrock Deposits of Lake Butler and Lake Fellmongery, South Australia. *Am. Mineral.* **2008**, *93*, 1014−1018.
(24) Chaliulina, R.Precipitated Calcium Carbonates Recycling Carbon Dioxide and Industrial Waste Brines, Doctor of Philosophy Thesis, The University of Aberdeen, 2019.
(25) Kimura, T.; Koga, N. Thermal Dehydration of Monohydrocalcite: Overall Kinetics and Physico-Geometrical Mechanisms. *J. Phys. Chem. A* **2011**, *115*, 10491−10501.
(26) Sun, R.; Willhammar, T.; Svensson Grape, E.; Strømme, M.; Cheung, O. Mesoscale Transformation of Amorphous Calcium Carbonate to Porous Vaterite Microparticles with Morphology Control. *Cryst. Growth Des.* **2019**, *19*, 5075−5087.
(27) Zhang, D.; Ghouleh, Z.; Shao, Y. Review on Carbonation Curing of Cement-Based Materials. *J. CO_2 Util.* **2017**, *112*, 119−131.
(28) Matschei, T.; Lothenbach, B.; Glasser, F. P. The AFm Phase in Portland Cement. *Cem. Concr. Res.* **2007**, *37*, 118−130.
(29) Matschei, T.; Lothenbach, B.; Glasser, F. P. Thermodynamic Properties of Portland Cement Hydrates in the System CaO-Al2O3-SiO2-CaSO4-CaCO3-H2O. *Cem. Concr. Res.* **2007**, *37*, 1379−1410.
(30) Zhang, D.; Cai, X.; Hu, L. Effect of Curing Temperature on Hydration of Calcium Aluminate Cement-Calcium Sulfate-Limestone System. *J. Mater. Civ. Eng.* **2018**, *30*, 1−7.
(31) Kaprálik, I.; Hanic, F. Phase Relations in the Subsystem C4A3SCSH2CHH2O of the System CaOAl2O3CSH2O Referred to Hydration of Sulphoaluminate Cement. *Cem. Concr. Res.* **1989**, *19*, 89−102.
(32) Yaseen, S. A.; Yiseen, G. A.; Li, Z. Elucidation of Calcite Structure of Calcium Carbonate Formation Based on Hydrated Cement Mixed with Graphene Oxide and Reduced Graphene Oxide. *ACS Omega* **2019**, *4*, 10160−10170.
(33) Menadi, B.; Kenai, S.; Khatib, J.; Aït-Mokhtar, A. Strength and Durability of Concrete Incorporating Crushed Limestone Sand. *Constr. Build. Mater.* **2009**, *23*, 625−633.
(34) Chen, J. J.; Kwan, A. K. H.; Jiang, Y. Adding Limestone Fines as Cement Paste Replacement to Reduce Water Permeability and Sorptivity of Concrete. *Constr. Build. Mater.* **2014**, *56*, 87−93.
(35) Ali, M.; Abdullah, M. S.; Saad, S. A. Effect of Calcium Carbonate Replacement on Workability and Mechanical Strength of Portland Cement Concrete. *Adv. Mater. Res.* **2015**, *1115*, 137−141.
(36) Yang, H.; Che, Y. Effects of Nano-CaCO 3 /Limestone Composite Particles on the Hydration Products and Pore Structure of Cementitious Materials. *Adv. Mater. Sci. Eng.* **2018**, *2018*, No. 5732352.
(37) Rodriguez-Blanco, J. D.; Shaw, S.; Bots, P.; Roncal-Herrero, T.; Benning, L. G. The Role of Mg in the Crystallization of Monohydrocalcite. *Geochim. Cosmochim. Acta* **2014**, *127*, 204−220.
(38) Maheswaran, S.; Ramachandra Murthy, A.; Ramesh Kumar, V.; Karunanithi, A. Characterisation Studies on the Particle Size Effect of Calcium Carbonate in High-Strength Concrete. *Mag. Concr. Res.* **2019**, *73*, 661−673.
(39) Pratiwi, W. D.; Triwulan; Ekaputri, J. J.; Fansuri, H. Combination of Precipitated-Calcium Carbonate Substitution and Dilute-Alkali Fly Ash Treatment in a Very High-Volume Fly Ash Cement Paste. *Constr. Build. Mater.* **2020**, *234*, No. 117273.
(40) McDonald, L. J.; Afzal, W.; Glasser, F. P. Evidence of Scawtite and Tilleyite Formation at Ambient Conditions in Hydrated Portland Cement Blended with Freshly-Precipitated Nano-Size Calcium Carbonate to Reduce Greenhouse Gas Emissions. *J. Build. Eng.* **2022**, *48*, No. 103906.
(41) McDonald, L. J.; Carballo-Meilan, M. A.; Chacartegui, R.; Afzal, W. The Physicochemical Properties of Portland Cement Blended with Calcium Carbonate with Different Morphologies as a Supplementary Cementitious Material. *J. Cleaner Prod.* **2022**, *338*, No. 130309.
(42) Rostami, V.; Shao, Y.; Boyd, A. J.; He, Z. Microstructure of Cement Paste Subject to Early Carbonation Curing. *Cem. Concr. Res.* **2012**, *42*, 186−193.
(43) Chen, T.; Gao, X. Effect of Carbonation Curing Regime on Strength and Microstructure of Portland Cement Paste. *J. CO_2 Util.* **2019**, *34*, 74−86.
(44) Zajac, M.; Lechevallier, A.; Durdzinski, P.; Bullerjahn, F.; Skibsted, J.; ben Haha, M. CO2 Mineralisation of Portland Cement: Towards Understanding the Mechanisms of Enforced Carbonation. *J. CO_2 Util.* **2020**, *38*, 398−415.
(45) Zajac, M.; Lechevallier, A.; Durdzinski, P.; Bullerjahn, F.; Skibsted, J.; Ben Haha, M. CO2 Mineralisation of Portland Cement: Towards Understanding the Mechanisms of Enforced Carbonation. *J. CO_2 Util.* **2020**, *38*, 398−415.

https://doi.org/10.1021/acsomega.2c03977
ACS Omega 2022, 7, 36318−36329

(46) Zhang, D.; Ghouleh, Z.; Shao, Y. Review on Carbonation Curing of Cement-Based Materials. *J. CO_2 Util.* **2017**, *21*, 119−131.
(47) Ho, L. S.; Nakarai, K.; Ogawa, Y.; Sasaki, T.; Morioka, M. Effect of Internal Water Content on Carbonation Progress in Cement-Treated Sand and Effect of Carbonation on Compressive Strength. *Cem. Concr. Compos.* **2018**, *85*, 9−21.
(48) Benhelal, E.; Rashid, M. I.; Holt, C.; Rayson, M. S.; Brent, G.; Hook, J. M.; Stockenhuber, M.; Kennedy, E. M. The Utilisation of Feed and Byproducts of Mineral Carbonation Processes as Pozzolanic Cement Replacements. *J. Cleaner Prod.* **2018**, *186*, 499−513.

https://doi.org/10.1021/acsomega.2c03977
ACS Omega 2022, 7, 36318−36329